Structural, Electronic, Magnetic and Vibrational Properties of Full-Heusler Ir_2CrX (X = Si, Ge) Compounds

Gh. Forozani[a,*], F. Karami[a], and M. Moradi[b]

[a]Department of Physics, Payame Noor University, P.O. Box 19395-3697, Tehran, Iran

[b]Department of Physics, College of Sciences, Shiraz University, Shiraz 71946, Iran

(Received January 28, 2020; in final form February 4, 2020)

The structural, electronic, magnetic, and vibrational properties of full-Heusler compounds Ir_2CrSi and Ir_2CrGe based on the density functional theory are investigated. Ir_2CrSi is half-metallic ferromagnet at equilibrium lattice constant and preserves its half-metallic behavior under stress. Ir_2CrGe just represents half-metallicity under stress. For this reason, we changed the equilibrium lattice constant from $-4\%a_0$ to $+4\%a_0$ in a range of $a = (a_0 \pm x\%a_0)$, where $x = 1, 2, 3, 4$, and calculations were done for these new lattice parameters. In all of this interval Ir_2CrSi holds its half-metallic property. The dynamical stability at equilibrium lattice constant and under stress have been investigated. The Ir_2CrSi compound has dynamical stability at lattice constant $a = a_0 - 3\%a_0$ and $a = a_0 - 4\%a_0$. The estimated Curie temperatures of Ir_2CrSi and Ir_2CrGe at equilibrium lattice constant occur to be 616.3 K and 415.3 K, respectively.

DOI: 10.12693/APhysPolA.137.430

PACS/topics: full-Heusler alloys, electronic structure, magnetic properties, half-metal ferromagnetic, dynamical stability

1. Introduction

In ferromagnetic materials, spin polarization near the Fermi surface plays an important role in spintronics [1–7]. These materials attracted much attention, especially in magnetoelectronics [8], tunneling magnetic resonance (TMR) [9–11], and spin waves [12–14]. Therefore, half-metallic ferromagnetics (HMFs) are important materials for spintronics, because they have a band gap at the Fermi surface in one of the spin direction and this exhibits 100% spin polarization at the Fermi surface [15]. The Heusler alloys are highly regarded for technological applications because of their relatively high Curie temperature [16–18] compared to other half-metallic compounds [19]. Groot and his coworkers [20] predicted half-metallic ferromagnetism in the half Heusler compound NiMnSb. Up to now, many compounds with this property have been discovered. The Heusler compounds are divided into two groups: half-Heusler and full-Heusler compounds [21–26]. The general formulae for half-Heusler and full-Heusler compounds are XYZ and X_2YZ, respectively, where X and Y are transition metals and Z is one of the *sp* element from the III, IV, and V main groups. The full Heusler compounds crystallize in $L2_1$ structures in which four fcc lattices penetrate along the main diameter and each element is located in one of these fcc lattice. The half-Heuslers have $C1_b$ structure which is similar to the $L2_1$ structure, with no elements in one of the fcc lattice points. Birsan [27] investigated the electronic structure and magnetic properties of full-Heusler Zr_2CrAl and found that this compound is half metal with Hg_2CuTi structure and because of its high spin polarization it is a good candidate for polarized spin currents. In 2019 Boumia et al. [28] studied structural, electronic and magnetic properties of new full-Heusler alloys Rh_2CrZ (Z = Al, Ga, In). They used generalized gradient approximation (GGA-PBE), the Blaha modified Becke–Johnson (TB-mBJ) potential, and GGA+U. They showed that these compounds are stable in Cu_2MnAl-type structure and can be synthesized experimentally, the compound Rh_2CrZ (Z = Al, Ga) are half metal ferromagnets and they are suitable for spintronic applications. Krishnaveni [29] studied electronic structure, magnetic, half metallic, mechanical, and thermodynamic properties of Ir_2MnAl and Ir_2MnGa. He showed that these compounds are stable in ferromagnetic state and Ir_2MnAl is half metal. Iridium based Heusler alloys have been extensively reviewed, such as: Ir_2CrAl [30], Ir_2MnSi [31], Ir_2VGa and Ir_2VGe [32], Ir_2MnAl [33]. The rapid development of spintronics and magnetoelectronics has led to significant growth in the investigation of half-metallic ferromagnets. Iridium based binary alloys are used in spintronic devices, memory storage devices, giant magnetoresistance (GMR), and tunneling magnetic resonance (TMR). Iridium has one of the highest melting points (2739 K), so Ir and its alloys has been used as an antiferromagnetic layer in magnetic recording, spark plugs, dip pens, rings, and tooth fillings. In addition, electrical and electrochemical applications of Ir have increased [34].

In present study we want to examine structural, electronic, magnetic, and vibrational properties of Ir_2CrX (X = Si, Ge) compounds to consider whether these compounds are suitable in spintronic application.

*corresponding author; e-mail: forozani@pnu.ac.ir

2. Computational method

The calculations are done and performed based on the density functional theory (DFT), using the GGA method in the scheme of Perdew–Burke–Ernzerhof (PBE) [35]. We have used the QUANTUM ESPRESSO package [36] and PWscf method. The cut-off energy for wave function of 40 Ry and cut-off energy for charge density expansions of 400 Ry are considered. The K-point meshes of $12 \times 12 \times 12$ is used to model the first Brilouin zone. Also the q-point mesh of $2 \times 2 \times 2$ are used to obtain phonon dispersion curves and phonon density of states by using Quantum ESPRESSO. To achieve the self-consistency the convergence thresholds set as 10^{-7} a.u. for total energy.

3. Results and discussion

In order to find a stable structure for Ir_2CrSi and Ir_2CrGe compounds, two common structures for the proposed full-Heusler have been compared. Two possible types of structures for full-Heusler Ir_2CrSi alloy are indicated in Fig. 1 and the parameters are shown in Table I.

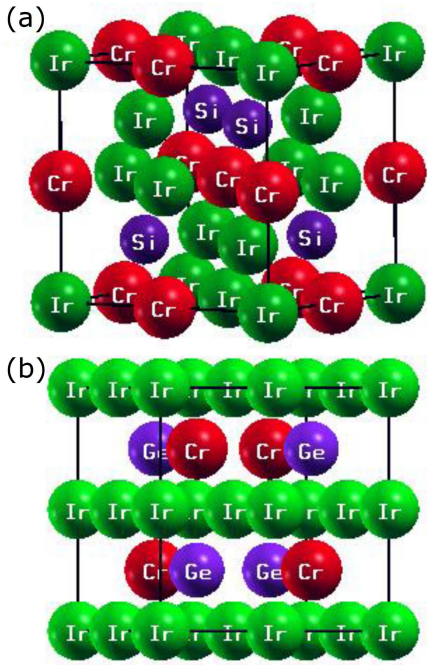

Fig. 1. Crystal structures of Ir_2CrSi full-Heusler alloy in (a) type a and (b) type b .

The possible atomic arrangement of Ir_2CrX. TABLE I

	Type a	Type b
Ir	(0,0,0)	(0,0,0)
Cr	(0.25,0.25,0.25)	(0.5,0.5,0.5)
Ir	(0.5,0.5,0.5)	(0.25,0.25,0.25)
X	(0.75,0.75,0.75)	(0.75,0.75,0.75)

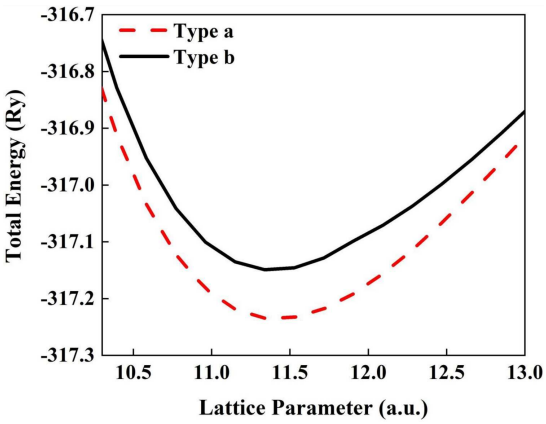

Fig. 2. Total energy as a function of lattice parameter (a.u. = atomic units) for two types of atomic arrangements of the Ir_2CrSi.

TABLE II

Equilibrium lattice parameter, bulk modulus, total magnetic moment and partial magnetic moments of Ir, Cr and X = Si, Ge.

Compd.	a [a.u.]	B [GPa]	M_{tot} [μ_{B}]	M_{Ir} [μ_{B}]	M_{Cr} [μ_{B}]	M_{X} [μ_{B}]
Ir_2CrSi	11.4772	203.7	3.94	0.4146	3.1219	0.0416
Ir_2CrGe	11.6834	188.3	3.92	0.3933	3.1487	0.0556

Figure 2 shows the total energy as a function of lattice parameter for Ir_2CrSi compound in type a and b structures for ferromagnetic state. As shown in Fig. 2, type a is the most stable structure. Therefore, we do the rest of the calculations with this stable structure for Ir_2CrX (X = Si, Ge). In this stable structure, the Ir atoms occupy A (0, 0, 0) and C (0.5, 0.5, 0.5) sites, Cr atom is in B (0.25, 0.25, 0.25) position and X atom is in D (0.75, 0.75, 0.75) position in the Wyckoff coordinates. The location of the Ir and Cr atoms depends on the number of their $3d$ electrons. Elements with more $3d$ electrons usually occupy the A and C sites and elements with fewer $3d$ electrons occupy B sites. For Ir_2CrX (X = Si, Ge), the Ir atoms have more valence electrons than Cr atom. Therefore, Ir tends to occupy A and C sites.

By fitting the total energy as a function of volume to the Murnaghan equation of state [37], equilibrium lattice parameter a, and bulk modulus B are calculated, as shown in Table II. Also the total moment and partial magnetic moments are listed in this table. Total magnetic moments do not exactly have integer values and have a magnitude of 3.92 μ_{B} for Ir_2CrGe and 3.94 μ_{B} for Ir_2CrSi. The latter exhibits half-metallic property at equilibrium lattice constant and half-metallic band gap is 0.105 eV. According to the Slater–Pauling rule [38], for full-Heusler alloys the total magnetic moment could be obtained from equation

$$M_{\mathrm{tot}} = (Z_{\mathrm{tot}} - 24)\,\mu_{\mathrm{B}}, \tag{1}$$

where Z_{tot} is the total number of valence electrons and μ_{B} is the Bohr magneton.

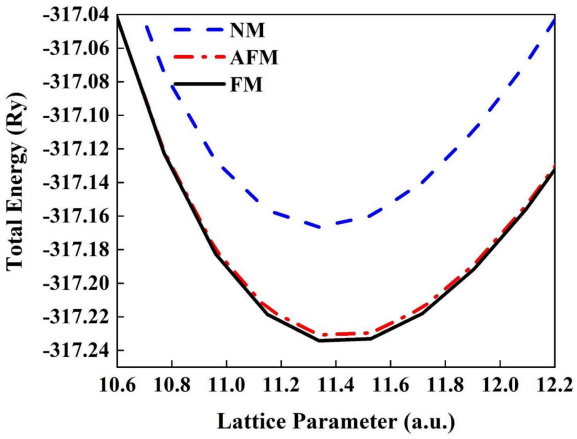

Fig. 3. Total energy as a function of lattice parameter in the FM, AFM, and NM states for the Ir_2CrSi at type a structure.

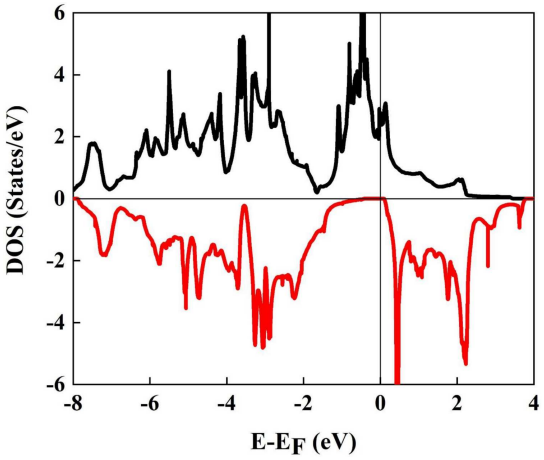

Fig. 4. Total DOS for Ir_2CrSi. Negative numbers on the vertical axis represent the minority spin states.

For the stable structure of type a, we have plotted the total energy in terms of lattice constant for the antiferromagnetic (AFM), ferromagnetic (FM), and non-magnetic (NM) states. As one can see in Fig. 3, ferromagnetic state has lower total energy than AFM and NM states. Therefore, ferromagnetic state is stable state for both compounds, however, it is slightly different than the antiferromagnetic state.

The possibility of experimental fabrication of these compounds have been investigated by calculating the cohesive energy. The cohesive energy (E_{coh}) is calculated using the following relation [39]:

$$E_{\rm coh} = \left(2E^{\rm Ir}_{\rm atom} + E^{\rm Cr}_{\rm atom} + E^{\rm X}_{\rm atom}\right) - E^{\rm Ir_2CrX}_{\rm total}, \qquad (2)$$

where E_{atom} is the total energy of isolated atom and E_{total} is the total energy of full-Heusler. When the cohesive energy is positive, the compound has structural stability. Cohesive energy is 23.77 eV and 22.09 eV for Ir_2CrSi and Ir_2CrGe, respectively, so they have structural stability.

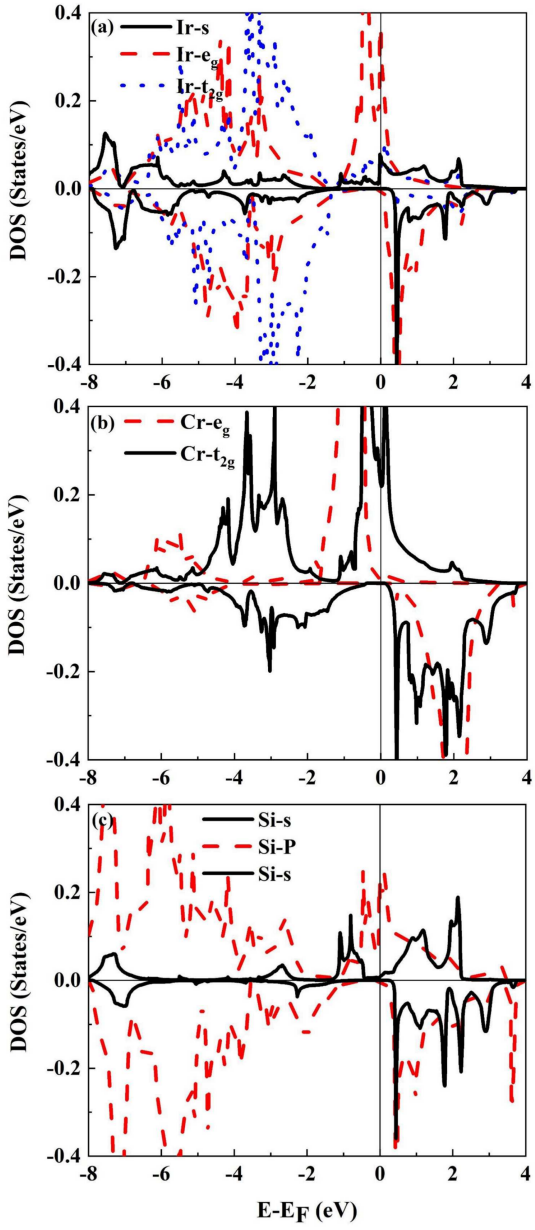

Fig. 5. Partial DOS for (a) Ir, (b) Cr, (c) Si, for Ir_2CrSi. Negative numbers on the vertical axis represent the minority spin states.

To investigate the physical properties of these compounds, we have considered the band structure and density of states here. The total density of states of Ir_2CrSi has been plotted in Fig. 4. As shown in this figure, the spin majority states have metallic behavior while spin minority states have insulator behavior. Therefore, Ir_2CrSi show a half-metallic behavior. Moreover, it means that the Fermi level is in the conduction band for spin up state and in the gap for spin down. Since the half-metallic gap for this compound is 0.105 eV and electron spin polarization P is 100% at the Fermi surface [40], Ir_2CrSi is a good candidate for spintronic applications. To investigate the

origin of half metallic ferromagnetic the partial density of states for this compound are plotted in Fig. 5. As seen in this figure, the half-metallic gap mainly caused by e_g and t_2 orbitals of Cr and Ir. As it is seen, the contribution of s electrons in the Ir, Cr, and Si density of states (DOS) is very small. The peaks in the total DOS, which are located below the E_F, correspond to hybridization of the d-orbital of Ir and Cr atoms. The peaks, which are located above E_F correspond to the anti-bonding state of Ir and Cr atoms. In equilibrium lattice constant the Ir_2CrGe has no half-metallic gap at the Fermi surface, and its electron spin polarization P is 99%.

According to Table II, for both compounds the largest contribution to total magnetic moment is due to the Cr which is very close to the total magnetic moment value. The band structure of Ir_2CrSi compound is plotted in Fig. 6. As it is visible, there is a gap in minority spin states, that shows the semiconductor behavior. There is a direct gap of 0.433 eV for minority spin channels at the Γ point.

The Curie temperature (T_C) is one of the important quantities for the applicability of a compound in spintronics. It is calculated by using the mean field approximation (MFA) as [41]:

$$T_C = \frac{2\Delta E_{AFM-FM}}{3k_B}, \tag{3}$$

where k_B is the Boltzmann constant and ΔE_{AFM-FM} is the energy difference between the antiferromagnetic and ferromagnetic states. The Curie temperature at equilibrium lattice constant is 616.3 K and 415.3 K for Ir_2CrSi and Ir_2CrGe, respectively. In fact, those are very good temperatures for spintronic applications.

To construct the spintronic devices, usually a layer of half-metallic materials is grown on a substrate of semiconductor [42]. In this process, the lattice constant of half-metallic materials may be changed and phase state transitions from ferromagnetic to nonmagnetic occur. The variation of the lattice parameter influences the spin polarization and magnetic moment. Thus, the investigation of the relationship between the half-metallic character of Ir_2CrX (X = Si, Ge) and the lattice parameter is useful. For this reason we changed lattice constant in the interval from -4 to $+4$ percent of the equilibrium lattice constant ($a = a_0 \pm x\%a_0$, $x = 1, 2, 3, 4$), and performed the calculations for density of states. The compound Ir_2CrSi in all ranges and the compound Ir_2CrGe in the range of $-2\%a_0$ to $-4\%a_0$, show half-metallic property. It seems that these full-Heusler alloys are suitable for growth on various semiconductor substrates to manufacture spintronic devices and spin valve.

Figure 7 shows the total magnetic moment of Ir_2CrSi in terms of lattice constants. As we can see, even for higher values of lattice constants, the magnitude of total magnetic moment is almost constant, and half-metallicity is preserved. When the lattice constant is smaller than 10.58 a.u., the reduction in the magnetic moment indicates the transition from ferromagnetism to nonmagnetic phase.

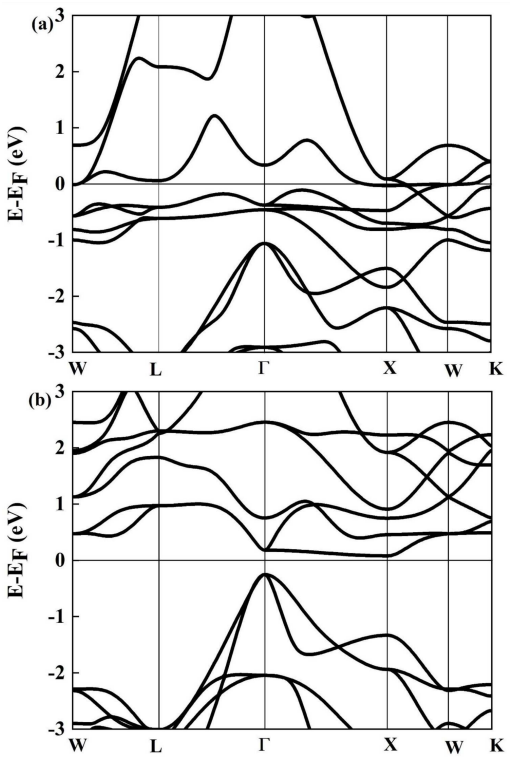

Fig. 6. Band structures for Ir_2CrSi (a) for spin up and (b) for spin down.

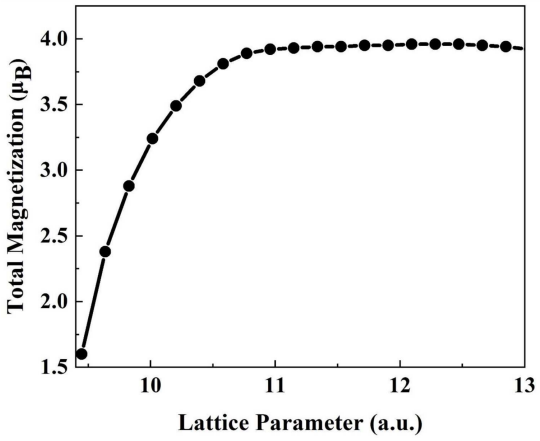

Fig. 7. Total magnetic moment (μ_B) as a function of lattice parameter for Ir_2CrSi.

The total magnetic moments and half-metallic gaps under different stresses for both compounds are listed in Table III. Also the total density of states for different stresses are plotted in Figs. 8 and 9. As we can see in Table III, for Ir_2CrSi the total magnetic momentum at this interval vary between 3.92 μ_B to 3.95 μ_B and the largest half-metallic gap is 0.129 eV at $a_0 + 3\%a_0$ lattice constant. We see that by increasing the lattice constant, the total magnetic moment increases. Also half metallic gap increases by increasing the lattice constant except

TABLE III

Energy of half metallic gap and total magnetic moment, under stress, for Ir_2CrX (X = Si, Ge) full-Heusler alloys.

Compounds under stress	E_{HM} [eV] Ir_2CrSi	E_{HM} [eV] Ir_2CrGe	M_{tot} [μ_B] Ir_2CrSi	M_{tot} [μ_B] Ir_2CrGe
$a_0 - 4\%a_0$	0.062	0.063	3.92	3.91
$a_0 - 3\%a_0$	0.075	0.077	3.93	3.91
$a_0 - 2\%a_0$	0.085	0.04	3.93	3.92
$a_0 - 1\%a_0$	0.096	–	3.94	3.92
a_0	0.105	–	3.94	3.92
$a_0 + 1\%a_0$	0.114	–	3.94	3.92
$a_0 + 2\%a_0$	0.121	-	3.95	3.92
$a_0 + 3\%a_0$	0.129	–	3.95	3.92
$a_0 + 4\%a_0$	0.053	–	3.95	3.92

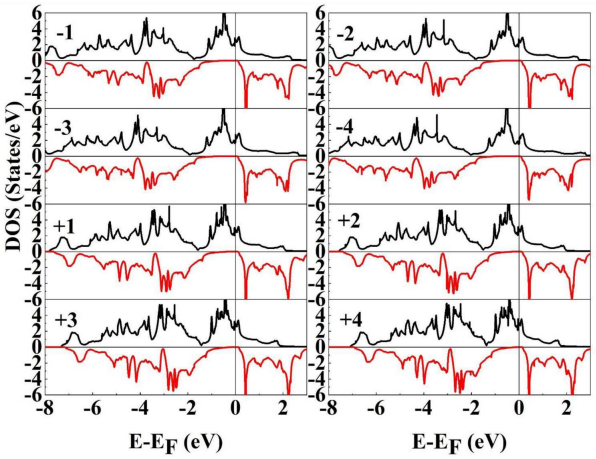

Fig. 8. Total DOS for Ir_2CrSi, under stress.

at $a_0+4\%a_0$ lattice constant. Thus Ir_2CrSi keeps its half-metallic properties under this stress. Ir_2CrGe has half-metallicity in the ranges of $a_0-2\%a_0$ to $a_0-4\%a_0$. In this interval the magnetic moment is 3.91 μ_B and 3.92 μ_B. The largest half-metallic gap is 0.077 eV at $a_0-3\%a_0$ lattice constant. In Table III one can see that Ir_2CrGe has no half-metallic gap from a_0 to $a_0+4\%a_0$. It means that with increase in the lattice constant the half-metallic gap is vanished. Comparing Ir_2CrGe with respect to Ir_2CrSi, one of the reasons could be that the atomic radius and atomic mass of Ge is larger than Si. Also, electron arrangements of Si and Ge are $3s^2 3p^2$ and $3d^{10}4s^2 4p^2$, respectively.

In this part at first the dynamical stability of Ir_2CrSi is investigated in equilibrium lattice constant and under stress. It is required to plot the phonon dispersion curves and phonon density of states. Since there are four atoms in the unit cell there are twelve phonon modes for any wave vector, three acoustical and nine optical branches. At the equilibrium lattice constant, the phonon frequency has negative value so it does not have dynamical stability. However, as shown in Fig. 10, this alloy has dynamical stability under stress at $a = a_0-3\%a_0$ and $a = a_0-4\%a_0$

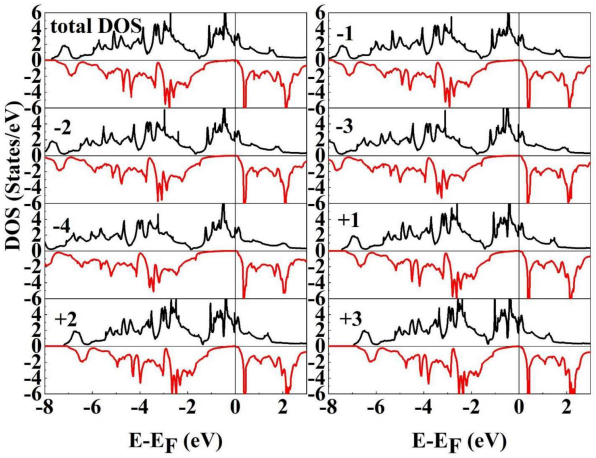

Fig. 9. Total DOS for Ir_2CrGe, at equilibrium lattice constant and under stress.

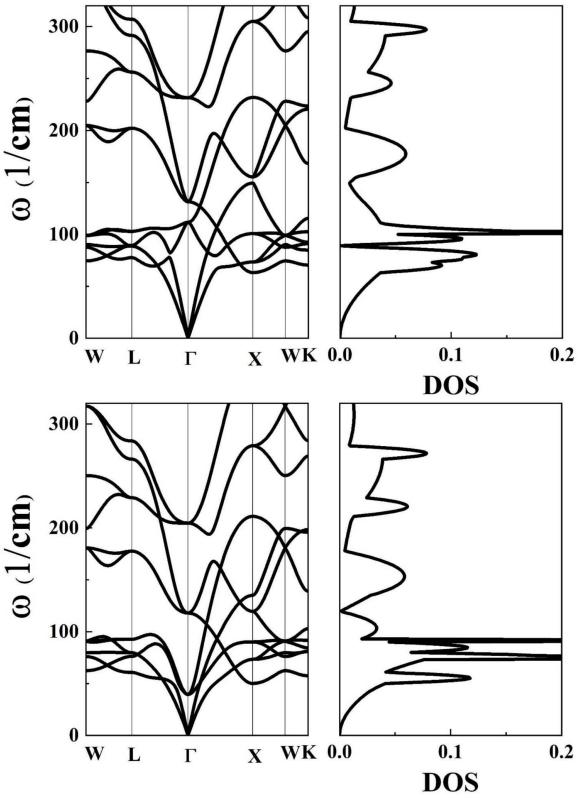

Fig. 10. The phonon dispersion curves and phonon total DOS for Ir_2CrSi at (a) $a = a_0 - 3\%a_0$ and (b) $a = a_0 - 4\%a_0$ lattice constants.

lattice constants. In this diagram all phonon frequencies are positive. We know that positive frequency indicates dynamical stability of the compound. We found that the dynamical stability exists at lowest lattice constant, lowest spin magnetization and lowest half-metallic gap, in the desired interval, which may show that this compound has more stability under stress.

4. Conclusions

The structural, electronic, magnetic, and phonon properties of full-Heusler compounds Ir_2CrX (X = Si, Ge) are investigated by using the first-principle calculations and GGA approximation. The calculated results show that the type a arrangement and ferromagnetic phase is most stable. The total magnetic moment was 3.94 μ_B and 3.92 μ_B for Ir_2CrSi and Ir_2CrGe, respectively. The Ir_2CrSi compound exhibits the half-metallic property. The half-metallic band gap of Ir_2CrSi was 0.105 eV. Also we investigated the half-metallicity and dynamical stability under stress in the intervals of $a = a_0 \pm x\%a_0$, $x = 1, 2, 3, 4$. We found that Ir_2CrSi preserve half-metallicity in all ranges and has dynamical stability at lattice constant equal to $a = a_0 - 3\%a_0$ and $a = a_0 - 4\%a_0$. The Ir_2CrGe compound shows the half-metallic property in a range of $a = a_0 - 2\%a_0$ to $a = a_0 - 4\%a_0$ lattice constant. The Curie temperatures of Ir_2CrSi and Ir_2CrGe are estimated at equilibrium lattice constants to be 616.3 K and 415.3 K, respectively. At equilibrium lattice constant and under stress Ir_2CrSi is half-metallic ferromagnet. Ir_2CrSi has 100% spin polarization and Ir_2CrGe has 99% spin polarization at the Fermi surface, so Ir_2CrX (X=Si, Ge) are suitable for spintronic devices.

References

[1] S.A. Wolf, D.D. Awschalom, R.A. Buhrman, J.M. Daughton, S.V. Molnar, M.L. Roukes, A.Y. Chtchelkanova, D.M. Treger, *Science* **294**, 1488 (2001).

[2] S.A. Khandy, D.C. Gupta, *J. Magn. Magn. Mater.* **441**, 166 (2017).

[3] S.A. Khandy, I. Islam, D.C. Gupta, A. Laref, *J. Solid State Chem.* **270**, 173 (2019).

[4] G.A. Prinz, *Phys. Today* **48**, 58 (1995).

[5] K.I. Kobayashi, T. Kimura, H. Sawada, K. Terakura, K. Tokura, *Nature* **395**, 677 (1998).

[6] J.H. Park, E. Vescovo, H.J. Kim, C. Kwon, R. Ramecsh, T. Venkatesan, *Nature* **392**, 794 (1998).

[7] S.J. Hashemifar, P. Kratzer, M. Scheffler, *Phys. Rev. Lett.* **94**, 096402 (2005).

[8] G. Prinz, *Science* **282**, 1660 (1998).

[9] P. Mavropoulos, M. Lezaic, S. Blugel, *Phys. Rev. B* **72**, 174428 (2005).

[10] M. Lezaic, P.H. Mavropoulos, J. Enkovaara, G. Bihlmayer, S. Bluge, *Phys. Rev. Lett.* **97**, 026404 (2006).

[11] S. Chadov, T. Graf, K. Chadova, X. Dai, F. Casper, G.H. Fecher, C. Felser, *Phys. Lett.* **107**, 047202 (2011).

[12] S. Li, C. Cheng, K. Meng, C. Chen, *Jpn. J. Appl. Phys.* **58**, 040903 (2019).

[13] L. Berger, *Phys. Rev. B* **54**, 9353 (1996).

[14] D.D. Stancil, A. Prabhakar, *Spin Waves: Theory and Applications*, Springer Sci. & Business Media LLC, 2009.

[15] R.A. de Groot, F.M. Mueller, P.G. van Engen, K.H.J. Buschow, *Phys. Rev. Lett.* **50**, 2024 (1983).

[16] I. Zutic, J. Fabian, S. Das Sarma, *Rev. Mod. Phys.* **76**, 323 (2004).

[17] H.H. Zenasni, I. Faraoun, C. Esling, *J. Magn. Magn. Mater.* **333**, 162 (2013).

[18] F. Casper, T. Graf, S. Chadov, B. Balke, C. Felser, *Semicond. Sci. Technol.* **27**, 10172 (2012).

[19] R. Shams Alam, M. Moradi, M. Rostami, H. Nikmanesh, R. Moayedi, Y. Bai, *J. Magn. Magn. Mater.* **381**, 1 (2015).

[20] R.A. De Groot, F.M. Mueller, P.G. van Engen, K.H.J. Buschow, *Phys. Rev. Lett.* **50**, 2024 (1983).

[21] I. Galanakis, P. Mavropoulos, *J. Phys. Condens. Matter* **19**, 315213 (2007).

[22] N. Kervan, S. Kervan, *Intermetallics* **37**, 88 (2013).

[23] N. Kervan, S. Kervan, *Intermetallics* **24**, 56 (2012).

[24] O. Canko, F. Taşkin, M. Atiş, N. Kervan, S. Kervan, *J. Supercond. Nov. Magn.* **29**, 1 (2016).

[25] M. Moradi, N. Taheri, M. Rostami, *Phys. Lett. A* **382**, 3004 (2018).

[26] M. Safavi, M. Moradi, M. Rostami, *J. Superconduct. Nov. Magn.* **30**, 989 (2016).

[27] A. Birsan, *Curr. Appl. Phys.* **14**, 1434 (2014).

[28] L. Boumia, F. Dahmane, B. Doumi, D.P. Rai, S.A. Khandy, H. Khachai, H. Meradji, A.H. Reshak, R. Khenata, *Chin. J. Phys.* **59**, 281 (2019).

[29] S. Krishnaveni, *Mater. Res. Express* **6**, 096545 (2019).

[30] S. Krishnaveni, M. Sundareswari, M. Rajagopalan, *IOSR J. Appl. Phys.* **7**, 52 (2015).

[31] E.G. Özdemir, E. Eser, Z. Merdan, *Chin. J. Phys.* **56**, 1551 (2018).

[32] S. Krishnaveni, *J. Phys. Conf. Ser.* **1172**, 012041 (2019).

[33] H.C. Kandpal, G.H. Fecher, C. Felser, *J. Phys. D Appl. Phys.* **40**, 1507 (2007).

[34] M. Hasani, A. Khodadadi, S.M.J. Koleini, A.H. Saeedi, A.M. Meléndez, *J. Phys. Conf. Ser.* **786**, 012042 (2017).

[35] J.P. Perdew, K. Burke, M. Ernzerhof, *Phys. Rev. Lett.* **77**, 3865 (1996).

[36] P. Giannozzi, S. Baroni, N. Bonini, *J. Phys. Condens. Matter* **21**, 395502 (2009).

[37] F.D. Murnaghan, *Proc. Natl. Acad. Sci. USA* **30**, 244 (1944).

[38] J. Kübler, *Physica B+C* **127**, 257 (1984).

[39] X.P. Wei, Y.D. Chu, X.W. Sun, J.B. Deng, Y.Z. Xing, *Superlatt. Microstruct.* **74**, 70 (2014).

[40] L. Zhang, Z.X. Cheng, X.T. Wang, R. Khenata, H. Rozale, *J. Superconduct. Nov. Magn.* **31**, 189 (2018).

[41] K. Sato, P.H. Dederichs, H. Katayama-Yoshida, J. Kudrnovský, *J. Phys. Condens. Matter.* **16**, S5491 (2004).

[42] M. Shaughnessy, R. Snow, L. Damewood, C.Y. Fong, *J. Nanomater.* **2011**, 140805 (2011).